RESEARCH ARTICLE

NANO · MICRO small
www.small-journal.com

Single-Molecule Electrical Conductance in Z-form DNA:RNA

Mauricio R. Aguilar, Jesus Jover, Eliseo Ruiz, Albert C. Aragonès, and Juan M Artés Vivancos**

Nucleic acids have emerged as new materials with promising applications in nanotechnology, molecular electronics, and biosensing, but their electronic properties, especially at the single-molecule level, are largely underexplored. The Z-form is an exotic left-handed helical oligonucleotide conformation that may be involved in critical biological processes such as the regulation of gene expression and epigenetic processes. In this work, the electrical conductance of individual Guanine Cytosine (GC)-rich DNA:RNA molecules is measured in physiological buffer and 2,2,2-Trifluoroethanol (TFE) solvent, corresponding to the natural (right-handed helix) A-form typical in DNA:RNA hybrids and the (left-handed) Z-form conformations, respectively. Single-molecule conductance measurements are performed using the Scanning Tunneling Microscopy (STM)-assisted break-junction method in the so-called "blinking" approach, recording the spontaneous formation of single-biomolecule junctions and performing statistical analysis of the signals. Circular Dichroism (CD) experiments and *ab initio* calculations are also done to rationalize the measured molecular conductivity with a simple structural and electronic model. These results show that the electrical conductivity of the Z-form is one order of magnitude lower than that of the more compact A-form. The longer molecular length and higher energy for the Highest Occupied Molecular Orbital (HOMO) of the Z-form account for the differences in single-molecule conductance observed experimentally.

1. Introduction

Nucleic acids are essential biomolecules[1] and important new materials for nanotechnology[2–5] due to their unique structural,[6] electronic,[7] and self-assembly properties.[8] Research has focused on both the mechanical[9,10] and electrical properties[11–21] of DNA and RNA, as well as the biological importance of these biomolecules. RNA has recently come into the spotlight of research for several reasons;[22] It plays a crucial role in gene expression,[23] regulating biochemical reactions,[24] acting as the messenger between DNA and ribosomes and proteins,[25] and also in immunological responses.[26,27] RNA can form hybrids with complementary DNA strands, which are essential for biological processes such as DNA replication,[28,29] transcription,[30] reverse transcription,[31] and more recently are an essential key for biotechnological tools in gene editing.[26,27] Although RNA and DNA are chemically similar, they differ in their bases and backbones. RNA contains uracil bases instead of thymine in DNA, and the backbones are different, with RNA having a ribose group instead of the deoxyribose that is present in DNA. RNA:DNA hybrids form a double helix similar to double-stranded (ds)DNA, and they can have different conformations. RNA:DNA hybrids are predominantly in the A-form (as is dsRNA), while dsDNA is mainly in the canonical B form.[32] In addition, local environment conditions can affect their conformation, and the oligonucleotides can be switched between these and to more exotic conformations, such as the left-handed Z-form.[33] The structural differences between these conformations make it feasible for the electronic overlap between

M. R. Aguilar, J. Jover, E. Ruiz
Departament de Química Inorgànica i Orgànica, Secció de Química Inorgànica
Universitat de Barcelona
Diagonal 645, Barcelona 08028, Spain

The ORCID identification number(s) for the author(s) of this article can be found under https://doi.org/10.1002/smll.202408459

[+]Present address: European Research Council Executive Agency (ERCEA), Brussels, Belgium

DOI: 10.1002/smll.202408459

M. R. Aguilar, J. Jover, E. Ruiz, A. C. Aragonès
Institut de Química Teòrica i Computacional (IQTC)
Diagonal 645, Barcelona 08028, Spain

A. C. Aragonès
Departament de Ciència de Materials i Química Física
Universitat de Barcelona
Marti i Franquès 1, Barcelona 08028, Spain
E-mail: acortijos@ub.edu

J. M Artés Vivancos[+]
Department of Chemistry
University of Massachusetts Lowell
Lowell, MA 01854, USA
E-mail: juan_artesvivancos@uml.edu

the π orbitals in the bases to vary, which could lead to substantial differences in the electronic and charge transport (CT) properties of RNA:DNA hybrids in different conformations.[17,18] It is important to explore the electronic properties of these systems for not only both molecular electronics[34] and biosensor applications,[35,36] but also because these properties may underlie biophysical properties and biological activity.

The Z-form may be the most intriguing and understudied of the possible oligonucleotide conformations. It has a distinct zigzag structure, which gives it its name. The Z-form is the only known left-handed form, slightly more elongated compared to the more common B-form[6] and can be found in both DNA and RNA.[33] Although research is ongoing to determine the exact biological role of the Z-form, it has been shown to be involved in regulation of gene expression,[37,38] and epigenetic processes.[39] With regard to its single-molecule electronic properties, a pioneering experimental work in dsDNA found that the Z-form has lower conductivity respect to the B-form.[40] Electrochemical approaches previously reported similar findings.[41] However, structural insights[33] and computational studies[42] have suggested that Z-form helices may support efficient CT. This is because the bases are only slightly more separated than in the B-form and may maintain adequate π stacking along the helix. Interestingly, an early study estimated that a Guanine Cytosine (GC)-rich elongated oligonucleotide, with well-aligned bases, could exhibit conductance that is approximately an order of magnitude higher than that of the B-form.[42] Although experimental reports in the last two decades have demonstrated progress characterizing the electronic properties of oligonucleotides at the single-molecule level,[15–21,35,40,43] much more research is needed to explore the rules behind the charge-transport mechanisms in nucleic acids.[34] Also, determining the single-molecule conductance of DNA:RNA hybrids in the Z-form is crucial since it is the prerequisite for emerging and future research in single-biomolecule spin filters based on oligonucleotide helices with different or switchable chiralities.

In this work, we measure the single-molecule electrical conductance of GC-rich DNA:RNA hybrid oligonucleotides in buffer and in 2,2,2-Trifluoroethanol (TFE) solvent, corresponding to the natural A-form and Z-form conformations, respectively. Our experimental results show that the electrical conductivity of the Z-form is lower than that of the A-form.[17,18] Structural determination and ab initio electronic calculations allow to rationalize these experimental result. These are the first single-molecule conductance experiments in a left-handed DNA:RNA oligonucleotide.

2. Results and Discussion

We perform single-molecule electrical measurements of different conformations of DNA:RNA hybrids with identical sequence (CC CGC GCG CCC and rGrGrG rCrGrC rGrCrG rGrG) using the Scanning Tunneling Microscope-assisted Break Junctions method (STM-BJ),[44] in the so-called "blinking" approach,[45] recording the spontaneous formation of single-biomolecule junctions.[46] These oligonucleotides can bind the gold electrodes thanks to the 5' and 3' thiol terminal (–SH) groups introduced in the DNA probe strand (see supporting methods and Figure S1, Supporting Information, for details), a common approach in single-molecule electrical conductivity experiments.[17–20,35] The conformation of the oligonucleotides is controlled by using different chemical environments for the experiments; experiments in physiological buffer favor the more compact right-handed A-form (**Figure 1A**), while experiments in TFE solvent induce the left-handed extended Z-form[47] (Figure 1B). These different conformations are well documented in the literature,[33] and we have further tested this using Circular Dichroism (CD) measurements on the oligonucleotides in the two different solvent conditions (see below).

Figure 1 shows these single-molecule conductance experiments. The setup displayed in 1A shows an idealized picture of the transient binding of the A-form DNA:RNA hybrid between the tip and the sample electrodes, while the electrical conductance in the junction is monitored in an experiment in buffer solution. In contrast, panel 1B shows the same situation for experiments performed on TFE solvent, which induces the Z-form in the oligonucleotides. The static STM-BJ blinking approach[46] was employed to characterise RNA:DNA hybrids conductance. Briefly, a distance between the STM electrodes is fixed by the tunneling current setpoint value. Once mechanical stability is reached, the microscope's feedback loop is turned off and the current versus time is recorded, monitoring the blinking events, which are telegraphic signals in the junction conductance caused by stochastic connections and disconnections between the electrodes and the molecule, resulting in an abrupt jump and fall of the current from and to the tunneling current (see supporting methods and supporting figures, Supporting Information, for more details and control experiments). Linear and semi-logarithmic conductance histograms are built by the accumulation of 80 of these individual blinks, in each case. Data acquisition is done using a NI-DAQmx/BNC-2110 (National Instruments analog-digital converter interface acquisition) and treated using a custom LabView code, and plotted with Matplotlib.[48] We quantify the conductance by fitting a Gaussian curve on the histogram (dark blue trace in Figure 1C,D).

Figure 1 shows the conductance histograms obtained from 80 blinking traces in each case. The A-form DNA:RNA experiments (Figure 1C) result in a conductance peak centered around $9.4 \pm 1.3 \cdot 10^{-4} G_0$, one order of magnitude higher than the one obtained for a comparable amount of traces in the TFE experiments in Figure 1D, corresponding to the Z-form DNA:RNA ($9.6 \pm 1.7 \cdot 10^{-5} G_0$), where $G_0 = 2e^2/h = 7.75 \times 10^{-5}$ A/V(S) is the quantum of conductance (e is the electron charge and h is the Planck constant). The conductance value for the A-form is in good agreement with previous reports for this oligonucleotide, and within the experimental error of the value obtained from A-form oligonucleotides single-molecule electrical conductance reports using the current-distance so-called "tapping" approach.[17,18,20] This indicates that the mechanical forces in the STM do not significantly disturb the contacted biomolecule's conformation. The good agreement of the A-form results with published data supports the reproducibility of the STM-BJ as a robust single-molecule conductance measurement also in biomolecules.[34,36] The difference in conductance between A- and Z-forms is not surprising since the Z-form is comparatively longer than the A-form. Measuring end-to-end the molecular structures from ab initio calculations (see below), one obtains around 4 nm for the A-form *versus* 4.7 nm for the Z-form (see **Figure 2** and 1). Regardless of the charge-transport mechanism, the conductance

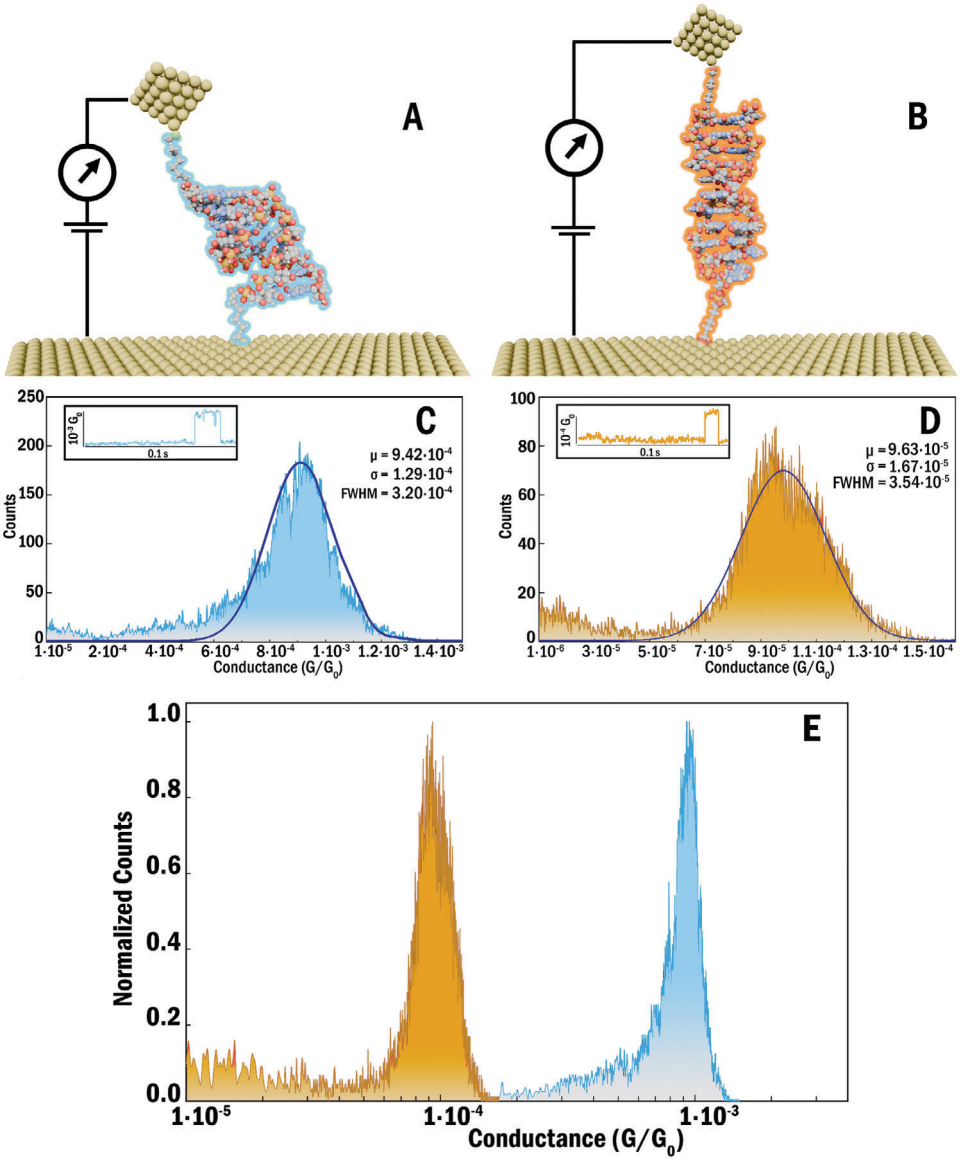

Figure 1. A,B) Diagrams of the experimental setup showing the RNA:DNA hybrids in the A- and Z-form, respectively, connected between two gold electrodes. C,D) Conductance histograms for the A- and Z-form of RNA:DNA hybrids in blue and orange, respectively. The dark blue traces are a gaussian fitting of the peak to obtain the indicated statistical values for the center and broadness of the distributions, specifically the mean conductance (μ), deviation (σ), and full width at half maximum (FWHM). A total of 80 blinks were collected for each sample. Insets show typical blinks for each form. Experiments were performed using a 10 nA V^{-1} amplifier and an applied bias voltage of 50 mV. The A- and Z-form were induced using 100 mM buffer solution (pH 7.4) or 2,2,2-Trifluoroethanol (TFE) solvent 60% in H_20 (v/v), respectively. E) Semi-logarithmic histograms for the A- and Z-form of RNA:DNA hybrids normalized to the total amount of accumulated current traces.

of an oligonucleotide generally decreases with the length of the molecule.[17,34,43] In fact, if one takes the distance decay factor (β) as the typical figure of merit for comparing molecules and biomolecules in molecular electronics, these measurements are consistent with $\beta = 0.2 - 0.3$ nm^{-1}, in line with previous reports of DNA and RNA conductance,[18] and with electrochemical results.[49] It is worth comparing the CT in the Z- *versus* the B-form with identical sequence,[17] surprisingly, the molecular conductance is similar. The Z-form in GC-rich DNA:RNA thus may have a more efficient charge transport process, taking into account its longer molecular length. This is in qualitative agreement with previous pioneering computational reports.[42] Comparing the histograms in Figure 1E, the histogram for the Z-form is also slightly broader than the one obtained for the A-form. This could be consistent with the A-form being more rigid than the Z-form, in an analogy with other single-molecule transport measurements comparing single-stranded *versus* double-stranded oligonucleotides, where the histograms also reflected information about biophysical properties such as molecular flexibility.[20]

We also perform Circular Dichroism (CD) experiments to confirm the conformations of these oligonucleotides in solution; the resulting spectra are shown in Figure 2. CD is a technique

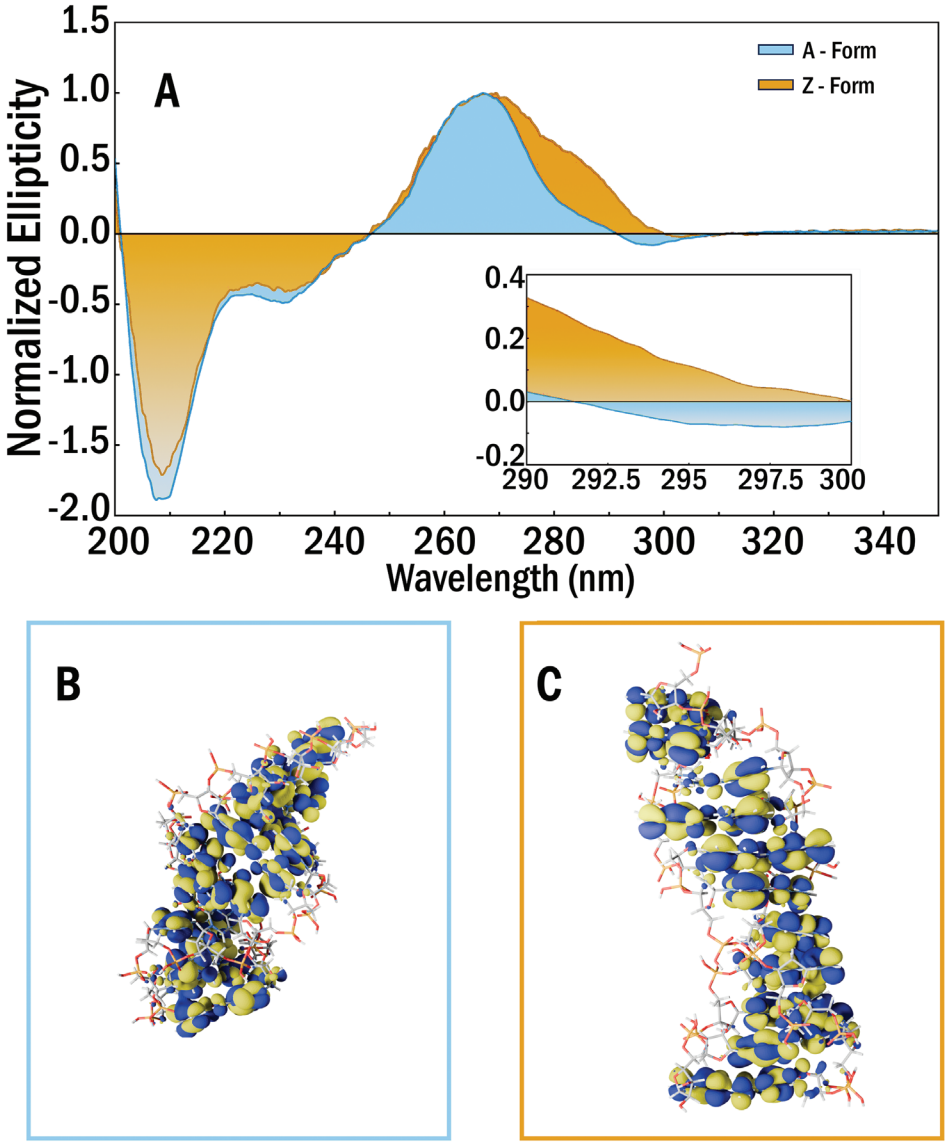

Figure 2. A) Circular dichroism spectra of A- and Z-form RNA:DNA hybrids. The inset shows a zoom in of the CD spectra around 295 nm. B,C) Results from DFT calculation: Isosurfaces of the occupied molecular orbitals close to the HOMO for A- and Z-form RNA:DNA hybrids, respectively. Isovalue = 2×10^{-2} au.

that allows the study of the chirality of biomolecules using circularly polarized light and is normally used to distinguish secondary structures such as right- or left-handed helices.[33] The spectra in Figure 2A agree with published results[33] and show that this DNA:RNA hybrid forms a left-handed helix in the TFE solvent,[33,50] while maintaining a right-handed A-form conformation in the spectra resulting from 100 mM phosphate buffer experiments. The inset in Figure 2A shows an enlarged version of the region of the CD considered to reflect left-handed or right-handed helicity in RNA oligonucleotides.[50] CD experiments in TFE result in spectra with positive ellipticity in the 290–300 nm range, consistent with published results for Z-form RNA oligonucleotides.[50] In contrast, CD spectra in buffer show negative ellipticities in this range, as expected for the A-form.[33] These results confirm the notion of measuring DNA:RNA in the left-handed Z-form in experiments in TFE *versus* the right-handed A-form in experiments in phosphate buffer.

Previous computational[51] and experimental[17] approaches have shown that single-molecule oligonucleotide conductance can be highly dependent on the conformation. To have more information about the CT process and to confirm the rationalization of the differences in conductance values, we turn to electronic structure calculations for these molecules. Briefly, A- and Z-form DNA:RNA hybrids are built with Avogadro[52] and the w3DNA[53] applet, respectively. In both cases, all the phosphate groups are protonated once to keep the fragments neutrally charged. Subsequently, geometries are optimized using the semi-empirical PM6 method[54] as implemented in Gaussian 16.[55] Finally, Gaussian 16 is employed to carry out single-point Density Functional Theory (DFT) calculations on the molecular

Table 1. Orbital energy levels (in eV), molecular length, and obtained experimental results: μ, σ, and FWHM of the different DNA:RNA forms.

	A Form	Z Form
HOMO	−5.01	−5.51
LUMO	−1.65	−1.98
GAP	3.35	3.53
Molecular Length	4.05	4.69
Average experimental conductance	9.42×10^{-4}	9.63×10^{-5}
σ	1.29×10^{-4}	1.67×10^{-5}
FWHM	3.20×10^{-4}	3.54×10^{-5}

structures, using the B3LYP[56–59] functional and the 6-31+G(d,p)[60–66] basis set for all the atoms, to obtain the molecular orbitals. Results are displayed in Figure 2.

Figure 2B,C shows the isosurfaces of the overlapping molecular orbitals close to the Highest Occupied Molecular Orbital (HOMO) for the A-form (from –6.23 to –5.01 eV) and the Z-form (from –6.67 to –5.51 eV) obtained from DFT calculations with an isovalue of 2×10^{-2} au. These orbitals seem to overlap over the whole structure in the case of the A-form oligonucleotide, probably favoring the electric conduction. On the other hand, the Z-form clearly shows regions where the occupied orbitals do not overlap (void spaces between some base pairs, see Figure 2C), which could be related to the worse conductance observed for this oligonucleotide. These results seem to be consistent with the higher electrical conductance obtained in the A-form experiments. Another factor to consider here is the energy of these orbitals. Since the HOMO is supposed to be the main mediator for the hopping CT process assumed to occur in oligonucleotides,[14,17,43] the energy value of this orbital is key, with higher values indicating enhanced conductance. **Table 1** shows the values obtained for the DFT calculations using the B3LYP/6-31+G(d,p) ensemble. Table 1 shows the Z-form HOMO around –5.51 eV, while the A-form is found at –5.01 eV, much closer to the energy level of the electrode injecting the charge in the molecular bridge (considering the Fermi energy of the electrodes in an electrolyte to be around –4.60 eV), resulting in a higher molecular conductance (see Figure 1). Previous work has shown that there may also be a significant tunneling contribution in short oligonucleotides,[17,43] even if the main mechanism is hopping considering the low distance decay factors. In that case, the tunneling barrier(s) will also be of important consideration. For this qualitative discussion, one could approximate that barrier to the molecular HOMO-LUMO gap obtained from the DFT calculations. The gap for the Z-form (3.53 eV in Table 1) is higher than that of the A-form (3.35 eV), which also supports a lower molecular conductance. In addition, as discussed above, the Z-form is known to be longer than the more compact A-form, and this should result in lower conductance. Most likely, all of these factors together contribute to the lower conductance observed in the Z-form.

3. Conclusion

In summary, all the structural and electronic results obtained from the simulations support the experimental finding of a lower molecular electronic conductance for the Z-form *versus* the A-form. This is in contrast with previous computational approaches suggesting a lower conductance for A-form oligonucleotides due to a poorer alignment of the orbital bases.[14] Both our experimental findings and DFT calculations, as well as previous combined experimental/computational reports,[17,18,20] show that the length of the molecule, the delocalization of the orbitals, and its energies are important for the molecular conductance and that the more compact A-form results in a higher conductance than longer molecular conformations. The longer Z-form shows a conductance slightly lower than the one reported for the B-form,[17,18] indicating a comparatively more efficient CT process in these longer GC-rich RNA left-handed oligonucleotides. Although this simple structural and electronic rationalization is sufficient to explain the molecular conductance findings, further single-molecule experiments and simulations are needed to discern the possible effect of the chirality of the helix,[67] if any. These results pave the way for spin-dependent single-molecule studies on these biomolecules that could result in groundbreaking molecular electronics applications.

4. Experimental Section

Reagents and Solution Preparation: A Goodfellow Au(111) single crystal was utilized as the STM sample electrode for the deposition of thiolated DNA:RNA oligonucleotide samples in solution. Before each experiment, the Au single crystal was cleaned using piranha solution. Complementary DNA probe (CC CGC GCG CCC) and RNA targets (rGrGrG rCrGrC rGrCrG rGrG) obtained from Biosynthesis inc (USA) were already modified on the 5' and 3' termini with C6 spacers and thiols linkers in the case of the DNA probe sequence. Once hybridized and desalted, the A-form or Z-form were induced using 100 mM phosphate buffer solution or TFE 60% in H_20 (v/v), respectively. Melting temperatures for the oligonucleotides were estimated to be between 57.2 and 59.7 °C using the IDT oligoanalyzer tool. The STM tips were coated with Apiezon wax (Apiezon) to insulate them from any leakage current caused by ions in the medium, thereby preventing interference with the molecular conductance measurements (see Supporting Information for more details).

Single-Molecule Conductance Measurements: Experiments were done using a Molecular Imaging Pico-STM head connected to a Digital Instruments Nanoscope IIIa controller with a 10 nA V^{-1} current preamplifier and bias voltage of 50 mV for all experiments. See Supporting Information for additional information and results from control experiments.

Circular Dichroism Measurements: All experiments were conducted using a JASCO J-1500 CD spectrometer equipped with a 1-mm path length quartz cell. Before each measurement, a blank spectrum (phosphate buffer or TFE) was collected and subtracted from the sample data. A 40 µL aliquot of a 150 mM oligonucleotide sample was added to the cell prior to spectrophotometry data collection. The final spectra were smoothed by averaging three scans.

Computational Details: A- and Z-form oligonucleotide hybrids were constructed using Avogadro[52] and the w3DNA[53] applet. In each case, all phosphate groups were protonated once to maintain a neutral charge on the fragments. The geometries were then optimized using the semi-empirical PM6 method implemented in Gaussian 16.[55] Finally, single-point DFT calculations were performed on the molecular structures using Gaussian 16, with the B3LYP functional and the 6-31+G(d,p) basis set applied to all atoms, to obtain the molecular orbitals. In order to plot the isosurfaces an isovalue of 2×10^{-2} au. was employed.

Statistical Analysis: For each experiment, blinks were manually collected using a customized LabView-based program.[68] Histogram plotting and calculation of mean conductance (μ), deviation (σ), and full width at half maximum (FWHM) using a Gaussian model were performed with

the Python libraries MatPLotLib[69] and LMFIT,[70] respectively. See Supporting Information for more details.

Supporting Information

Supporting Information is available from the Wiley Online Library or from the author.

Acknowledgements

M.R.A. thanks to the MICINN and the MdM program for the predoctoral grant PRE2019-089051. E.R. acknowledges the Generalitat de Catalunya for an ICREA Academia and 2021-SGR-00286 grants, and for computational resources to CSUC. A.C.A. thanks to the generous funding through the Max Planck Society. J.J. acknowledges the Universitat de Barcelona grant 2575QU02072030. This project was supported by the Spanish MCNU's PID2021-122464NB-I00, TED2021-129593B-I00, CNS2023-143773, and Maria de Maeztu CEX2021-001202-M projects. The views expressed are purely those of the authors and may not in any circumstances be regarded as stating an official position of the ERCEA and the European Commission.

Conflict of Interest

The authors declare no conflict of interest.

Data Availability Statement

The data that support the findings of this study are available from the corresponding author upon reasonable request.

Keywords

biomolecular electronics, biophysics, circular dichroism, DFT, DNA:RNA, molecular electronics, nanoscience, single-molecule conductance, solvent interactions, STM, Z-form

Received: September 17, 2024
Revised: December 6, 2024
Published online: December 18, 2024

[1] D. L. Nelson, A. L. Lehninger, M. M. Cox, *Lehninger principles of biochemistry*, Macmillan, **2008**.
[2] N. C. Seeman, *Nature* **2003**, *421*, 427.
[3] P. W. Rothemund, *Nature* **2006**, *440*, 297.
[4] T. J. Morrow, M. Li, J. Kim, T. S. Mayer, C. D. Keating, *Science* **2009**, *323*, 352.
[5] T. Wang, R. Sha, R. Dreyfus, M. E. Leunissen, C. Maass, D. J. Pine, P. M. Chaikin, N. C. Seeman, *Nature* **2011**, *478*, 225.
[6] J. D. Watson, F. H. Crick, *Nature* **1953**, *171*, 737.
[7] C. Dekker, M. Ratner, *Phys. World* **2001**, *14*, 29.
[8] Z. Dai, H. M. Leung, P. K. Lo, *Small* **2017**, *13*, 1602881.
[9] S. B. Smith, L. Finzi, C. Bustamante, *Science* **1992**, *258*, 1122.
[10] M. Rief, H. Clausen-Schaumann, H. E. Gaub, *Nature Struct. Biology* **1999**, *6*, 346.
[11] H.-W. Fink, C. Schönenberger, *Nature* **1999**, *398*, 407.
[12] D. Porath, A. Bezryadin, S. De Vries, C. Dekker, *Nature* **2000**, *403*, 635.
[13] K.-H. Yoo, D. Ha, J.-O. Lee, J. Park, J. Kim, J. Kim, H.-Y. Lee, T. Kawai, H. Y. Choi, *Phys. Rev. Lett.* **2001**, *87*, 198102.
[14] R. G. Endres, D. L. Cox, R. R. Singh, *Rev. Mod. Phys.* **2004**, *76*, 195.
[15] B. Xu, Zhang, X. Li, Tao, *Nano Lett.* **2004**, *4*, 1105.
[16] J. Hihath, B. Xu, P. Zhang, N. Tao, *Proc. Natl. Acad. Sci. USA* **2005**, *102*, 16979.
[17] J. M. Artés, Y. Li, J. Qi, M. Anantram, J. Hihath, *Nature Commun.* **2015**, *6*, 1.
[18] Y. Li, J. M. Artes, J. Qi, I. A. Morelan, P. Feldstein, M. P. Anantram, J. Hihath, *J. Phys. Chem. Lett.* **2016**, *7*, 1888.
[19] Y. Li, J. M. Artés, J. Hihath, *Small* **2016**, *12*, 432.
[20] S. Chandra, K. G. G. P. Arachchillage, E. Kliuchnikov, F. Maksudov, S. Ayoub, V. Barsegov, J. M. Artes Vivancos, *Nanoscale* **2022**, *14*, 2572.
[21] S. Chandra, A. Williams, F. Maksudov, E. Kliuchnikov, K. G. Pattiya Arachchillage, P. Piscitelli, A. Castillo, K. A. Marx, V. Barsegov, J. M. Artes Vivancos, *Sci. Rep.* **2023**, *13*, 19858.
[22] T. Pederson, *The Catalyst: RNA and the Quest to Unlock Life's Deepest Secrets*, W. W. Norton & Co Inc, New York **2024**, 2024.
[23] A. P. McCaffrey, L. Meuse, T.-T. T. Pham, D. S. Conklin, G. J. Hannon, M. A. Kay, *Nature* **2002**, *418*, 38.
[24] I. R. Lehman, M. J. Bessman, E. S. Simms, A. Kornberg, *J. Biol. Chem.* **1958**, *233*, 163.
[25] F. Crick, L. Barnett, S. Brenner, R. J. Watts-Tobin, *Nature* **1961**.
[26] E. Pennisi, *The Crispr Craze, Science* **2013**, *341*, 833.
[27] R. Barrangou, *Science* **2014**, *344*, 707.
[28] K. G. Lark, *J. Mol. Biol.* **1972**, *64*, 47.
[29] A. Kornberg, T. A. Baker, *DNA replication*, WH Freeman San Francisco, **1980**.
[30] P. F. Agris, *Nucleic Acids Res.* **2004**, *32*, 223.
[31] A. Telesnitsky, S. Goff, In: *Retroviruses*, Cold Spring Harbor Laboratory Press, Cold Spring Harbor (NY), **2011**.
[32] M. Egli, N. Usman, A. Rich, *Biochemistry* **1993**, *32*, 3221.
[33] J. Kypr, I. Kejnovská, D. Renčiuk, M. Vorlíčková, *Nucleic Acids Res.* **2009**, *37*, 1713.
[34] K. G. G. P. Arachchillage, S. Chandra, A. Piso, T. Qattan, J. M. A. Vivancos, *J. Mater. Chem. B* **2021**, *9*, 6994.
[35] Y. Li, J. Artés, E. Oren, H. Mohammad, M. Anantram, M. Alangari, S. Gokce, B. Demir, J. Hihath, **2018**.
[36] A. Williams, M. R. Aguilar, K. G. Pattiya Arachchillage, S. Chandra, S. Rangan, S. Ghosal Gupta, J. M. Artes Vivancos, *ACS Sustain. Chem. Eng.* **2024**.
[37] A. Rich, A. Nordheim, A. H.-J. Wang, *Annu. Rev.* **1984**, *53*, 791.
[38] D.-B. Oh, Y.-G. Kim, A. Rich, *Proc. Natl. Acad. Sci. USA* **2002**, *99*, 16666.
[39] T. Zhang, C. Yin, A. Fedorov, L. Qiao, H. Bao, N. Beknazarov, S. Wang, A. Gautam, R. M. Williams, J. C. Crawford, S. Peri, V. Studitsky, A. A. Beg, P. G. Thomas, C. Walkley, Y. Xu, M. Poptsova, A. Herbert, S. Balachandran, *Nature* **2022**, *606*, 594.
[40] K. Wang, J. M. Hamill, B. Wang, C. Guo, S. Jiang, Z. Huang, B. Xu, *chem. Sci.* **2014**, *5*, 3425.
[41] E. M. Boon, J. K. Barton, *Bioconjugate Chem.* **2003**, *14*, 1140.
[42] Y. A. Berlin, A. A. Voityuk, M. A. Ratner, *ACS nano* **2012**, *6*, 8216.
[43] L. Xiang, J. L. Palma, C. Bruot, V. Mujica, M. A. Ratner, N. Tao, *Nat. Chem.* **2015**, *7*, 221.
[44] B. Xu, N. J. Tao, *science* **2003**, *301*, 1221.
[45] A. C. Aragones, N. L. Haworth, N. Darwish, S. Ciampi, E. J. Mannix, G. G. Wallace, I. Diez-Perez, M. L. Coote, *Nature* **2016**, *531*, 88.
[46] W. Haiss, R. J. Nichols, H. van Zalinge, S. J. Higgins, D. Bethell, D. J. Schiffrin, *Phys. Chem. Chem. Phys.* **2004**, *6*, 4330.
[47] V. I. Ivanov, E. E. Minyat, *Nucleic Acids Res.* **1981**, *9*, 4783.
[48] J. D. Hunter, *Comput. Sci. Eng.* **2007**, *9*, 90.
[49] C. H. Wohlgamuth, M. A. McWilliams, J. D. Slinker, *Anal. Chem.* **2013**, *85*, 8634.

[50] T. Miyahara, H. Nakatsuji, H. Sugiyama, *J. Phys. Chem. A* **2016**, *120*, 9008.
[51] E. Starikov, A. Quintilla, K. Lee, W. Wenzel, *J. Chem. Phys.* **2008**, *129*, 13.
[52] M. D. Hanwell, D. E. Curtis, D. C. Lonie, T. Vandermeersch, E. Zurek, G. R. Hutchison, *J. Cheminform.* **2012**, *47*, W26.
[53] S. Li, W. K. Olson, X.-J. Lu, *Nucleic Acids Res.* **2019**, *47*, W26.
[54] J. J. P. Stewart, *J. Mol. Model.* **2007**, *13*, 1173.
[55] M. J. Frisch, G. W. Trucks, H. B. Schlegel, G. E. Scuseria, M. A. Robb, J. R. Cheeseman, G. Scalmani, V. Barone, G. A. Petersson, H. Nakatsuji, X. Li, M. Caricato, A. V. Marenich, J. Bloino, B. G. Janesko, R. Gomperts, B. Mennucci, H. P. Hratchian, J. V. Ortiz, A. F. Izmaylov, J. L. Sonnenberg, D. Williams-Young, F. Ding, F. Lipparini, F. Egidi, J. Goings, B. Peng, A. Petrone, T. Henderson, D. Ranasinghe, et al., Gaussian 16 Revision C.01, Gaussian Inc. Wallingford CT, **2016**.
[56] A. D. Becke, *Phys. Rev. A* **1988**, *38*, 3098.
[57] S. H. Vosko, L. Wilk, M. Nusair, *Can. J. Phys.* **1980**, *58*, 1200.
[58] C. Lee, W. Yang, R. G. Parr, *Phys. Rev. B* **1988**, *37*, 785.
[59] B. Miehlich, A. Savin, H. Stoll, H. Preuss, *Chem. Phys. Lett.* **1989**, *157*, 200.
[60] R. Ditchfield, W. J. Hehre, J. A. Pople, *J. Chem. Phys.* **1971**, *54*, 724.
[61] W. J. Hehre, R. Ditchfield, J. A. Pople, *J. Chem. Phys.* **1972**, *56*, 2257.
[62] P. C. Hariharan, J. A. Pople, *Theoretica Chim. Acta* **1973**, *28*, 213.
[63] M. M. Francl, W. J. Pietro, W. J. Hehre, J. S. Binkley, M. S. Gordon, D. J. DeFrees, J. A. Pople, *J. Chem. Phys.* **1982**, *77*, 3654.
[64] J. S. Binkley, M. S. Gordon, J. A. Pople, W. J. Pietro, W. J. Hehre, *J. Am. Chem. Soc.* **1982**, *104*, 2797.
[65] T. Clark, J. Chandrasekhar, G. W. Spitznagel, P. V. R. Schleyer, *J. Comput. Chem.* **1983**, *4*, 294.
[66] G. W. Spitznagel, T. Clark, P. von Ragué Schleyer, W. J. Hehre, *J. Comput. Chem.* **1987**, *8*, 1109.
[67] T. J. Zwang, S. Hurlimann, M. G. Hill, J. K. Barton, *J. Am. Chem. Soc.* **2016**, *138*, 15551.
[68] A. C. Aragonès, K. F. Domke, *Cell Reports Physical Science* **2021**, *2*, 4.
[69] J. D. Hunter, *Comput. Sci. Eng.* **2007**, *9*, 90.
[70] M. Newville, R. Otten, A. Nelson, T. Stensitzki, A. Ingargiola, D. Allan, A. Fox, F. Carter, Michał, R. Osborn, D. Pustakhod, S. Weigand, lneuhaus, A. Aristov, Glenn, Mark, mgunyho, C. Deil, A. L. R. Hansen, G. Pasquevich, L. Foks, N. Zobrist, O. Frost, Stuermer, J.-C. Jaskula, S. Caldwell, P. Eendebak, M. Pompili, J. H. Nielsen, A. Persaud, lmfit/lmfit-py: 1.3.2, Zenodo **2024**.

